



저작자표시-동일조건변경허락 2.0 대한민국

이용자는 아래의 조건을 따르는 경우에 한하여 자유롭게

- 이 저작물을 복제, 배포, 전송, 전시, 공연 및 방송할 수 있습니다.
- 이차적 저작물을 작성할 수 있습니다.
- 이 저작물을 영리 목적으로 이용할 수 있습니다.

다음과 같은 조건을 따라야 합니다:



저작자표시. 귀하는 원저작자를 표시하여야 합니다.



동일조건변경허락. 귀하가 이 저작물을 개작, 변형 또는 가공했을 경우에는, 이 저작물과 동일한 이용허락조건하에서만 배포할 수 있습니다.

- 귀하는, 이 저작물의 재이용이나 배포의 경우, 이 저작물에 적용된 이용허락조건을 명확하게 나타내어야 합니다.
- 저작권자로부터 별도의 허가를 받으면 이러한 조건들은 적용되지 않습니다.

저작권법에 따른 이용자의 권리는 위의 내용에 의하여 영향을 받지 않습니다.

이것은 [이용허락규약\(Legal Code\)](#)을 이해하기 쉽게 요약한 것입니다.

[Disclaimer](#)

A Thesis

for the Degree of Master of Science in Medicine

**Protective effects of 6'-O-galloylpaeoniflorin
against ultraviolet B radiation-induced
keratinocyte damage**

Yao Cheng Wen

Department of Medicine

Graduate School

Jeju National University

August, 2014

UVB에 의한 피부세포 손상에 대한 6'-O-galloylpaeoniflorin의 보호효과




지도교수 현진원

요정문

이 논문을 의학 석사학위 논문으로 제출함

2014년 8월

요정문의 의학 석사학위 논문을 인준함

심사위원장 고영상 
위 원 강희경 
위 원 현진원 

제주대학교 대학원

2014년 8월

**Protective effects of 6'-O-galloylpaeoniflorin
against ultraviolet B radiation-induced
keratinocyte damage**


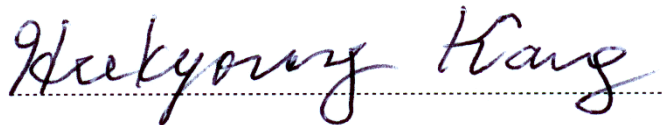

Yao Cheng Wen

(Advised by Professor Jin-Won Hyun)

A thesis submitted in partial fulfillment of the requirement
for the degree of Master of Science in Medicine

2014. 08.

This thesis has been examined and approved


.....

.....

.....

.....2014. 07. 04.....

Department of Medicine

GRADUATE SCHOOL

JEJU NATIONAL UNIVERSITY

ABSTRACT

The cytoprotective effects of isolated 6'-O-galloypaeoniflorin (GPF) against injury and death of human HaCaT keratinocytes resulting from ultraviolet B radiation were investigated. 6'-O-galloypaeoniflorin exhibited the capacity to scavenge intracellular reactive oxygen species (ROS) generated by ultraviolet B radiation. 6'-O-galloypaeoniflorin also attenuated ultraviolet B-induced oxidative macromolecular damage to DNA, lipids, and proteins, decreasing the number of DNA strand breaks, the level of 8-isoprostane (a biomarker of lipid peroxidation), and the level of protein carbonylation. Moreover, 6'-O-galloypaeoniflorin rescued HaCaT cells from ultraviolet B-induced cell death, by down-regulating the mitochondrial apoptotic pathway. Taken together, these results indicate that 6'-O-galloypaeoniflorin has the potential to be developed as a medical agent against ROS-mediated skin diseases.

CONTENTS

ABSTRACT.....	i
CONTENTS.....	ii
LIST OF FIGURES	iv
1. Introduction.....	1
2. Materials and Methods.....	3
2-1. Materials.....	3
2-2. Cell culture	4
2-3. UV/visible light absorption analysis	4
2-4. Detection of intracellular ROS	4
2-5. Single-cell gel electrophoresis (comet assay).....	5
2-6. Lipid peroxidation assay	6
2-7. Protein carbonyl formation.....	6
2-8. Cell viability assay	6
2-9. Nuclear staining with Hoechst 33342.....	7
2-10. Detection of sub-G1 hypodiploid cells.....	7
2-11. Terminal deoxynucleotidyl transferase-mediated digoxigenin-dUTP nick end labeling (TUNEL) assay	7
2-12. Western blot analysis.....	8

2-13. Statistical analysis	8
3. Results.....	9
3-1. GPF absorbs UVB rays	9
3-2. GPF scavenges ROS induced by UVB irradiation in HaCaT keratinocytes.....	10
3-3. GPF attenuates UVB-induced macromolecular damage in HaCaT cells	13
3-4. GPF protects HaCaT cells against apoptosis induced by UVB radiation.....	18
3-5. GPF prevents UVB-induced HaCaT cell death by regulating the mitochondria- related apoptotic pathway	23
4. Discussion	25
5. References.....	29
6. Abstract in Korean	34
7. Acknowledgement.....	35

LIST OF FIGURES

FIGURE 1. GPF absorbs UVB light.

- (A) Chemical structure of GPF.....3
- (B) UV/visible spectroscopic measurements were conducted in the spectral range from 250 to 400 nm9

FIGURE 2. GPF attenuates intracellular ROS generation in HaCaT cells.

- (A) Intracellular ROS were detected by flow cytometry after DCF-DA staining 11
- (B) Intracellular ROS levels were analyzed by spectrofluorometry after DCF-DA staining 12
- (C) Intracellular ROS levels were detected by confocal microscopy after DCF-DA staining 12

FIGURE 3. GPF protects HaCaT cells against UVB-induced oxidative DNA, lipid, and protein damage.

- (A) The comet assay was performed to assess DNA damage..... 14
- (B) Lipid peroxidation was assayed by measuring 8-isoprostane levels in conditioned medium 16
- (C) Lipid peroxidation was assayed by measuring lipid hydroperoxide detection via fluorescence microscopy after the DPPH reaction 16
- (D) Protein oxidation was assayed by measuring the amount of carbonyl formation 17

FIGURE 4. GPF prevents cell death and apoptosis induced by UVB radiation.

- (A) Cell viability was determined by the MTT assay after treated with 20 μ M GPF or 2 mM NAC, and then exposed to UVB radiation..... 18
- (B) Apoptotic bodies in cells stained with Hoechst 33342 dye were observed by

fluorescence microscopy and quantitated.....	20
(C) Sub-G1 cells were detected by flow cytometry after PI staining	21
(D) Apoptotic cells were detected by the TUNEL staining assay and quantified.....	22

FIGURE 5. Effects of GPF on proteins related to mitochondrial apoptosis, as determined by Western blotting.

(A) Cell lysates were electrophoresed, and cleaved caspase 9, cleaved caspase 3, cleaved PARP were detected using the appropriate antibodies	24
(B) Cell lysates were electrophoresed, and Bcl-2, and Bax were detected using the appropriate antibodies.....	24

1. Introduction

Chronic or repeated UVB exposure of human skin can cause severe skin damage, including photo-aging, inflammation, and photo-carcinogenesis (Liu et al. 2012; Sander et al. 2004). The predominant type of direct photochemical damage to cellular DNA involves absorption of UVB photons by the bases, mostly the pyrimidines (thymine, cytosine, and the minor 5-methylcytosine) and to a lesser extent the purines (Ravanat et al. 2001). Moreover, the toxic effects of UVB are further aggravated by the photosensitizing actions of exogenous and endogenous chromophores, which generate harmful reactive oxygen species (ROS) in skin cells (Hyun et al. 2012).

UVB radiation induces ROS generation in irradiated cells by activating molecules such as riboflavin, tryptophan, and porphyrin, which can then activate cellular oxygen (Ikehata and Ono 2011). Under normal circumstances, ROS play a critical role in mediating cell fate by initiating responses appropriate for cell survival, acting as signaling molecules in pathways involved in regulation of gene stability, and altering transcription via effects on chromatin stability (Alfadda and Sallam 2012). However, excess UVB-induced ROS can disrupt the balance between intracellular ROS and the antioxidant defense system of the irradiated cell, thereby overwhelming its antioxidant capacity and causing oxidative stress (Scandalios 2002). Oxidative stress jeopardizes the integrity of the oxidizable structures that are critical for cell homeostasis, resulting in oxidative photo-lesions of macromolecules (DNA, proteins, and lipids) in the skin (F'guyer et al. 2003). Furthermore, oxidative stress induced by UVB radiation triggers apoptosis, which is a form of programmed cell death (Hampton and Orrenius 1998). Hence, upon exposure to UVB light, the resultant oxidative stress causes damage to biomolecules and affects the integrity of cells and tissues (Stahl and Sies 2002). Photo-oxidative damage plays a critical role in pathological processes and the development

of disorders that affect the skin. Therefore, the use of antioxidants may be a valuable strategy to contend with UVB-induced cutaneous lesions and diseases.

Recently, natural agents with potential antioxidant, anti-inflammatory, anti-mutagenic, anti-carcinogenic, and immune-modulatory properties have attracted considerable attention as agents that could be used to prevent UV-induced skin damage (Afaq 2011). Such compounds have the ability to exert striking inhibitory effects on diverse cellular and molecular events. A growing body of evidence indicates that natural antioxidants safeguard cutaneous cells and tissues against damage triggered by UVB radiation. In one study, intracellular accumulation of ascorbic acid, the main physiological water-soluble vitamin, resulted in significant protection against UVB-induced cell death in human HaCaT keratinocytes (Savini et al. 1999).

In this study, the cytoprotective properties of 6'-O-galloylpaeoniflorin (GPF) against the deleterious effects of UVB in HaCaT cells were assessed. GPF, which consists of D-glucose, galloyl, and benzoyl moieties, is an acylated monoterpene glucoside isolated from the peony plant (*Paeoniae lactiflorae* Pall) (Kang et al. 1991). GPF exhibits androgen receptor-binding activity and inhibits the growth of androgen-dependent prostate cancer cell line (Washida et al. 2009). Furthermore, GPF is a more potent scavenger of the 1,1-diphenyl-2-picrylhydrazyl radical than α -tocopherol, and its galloyl group is essential for its ability to scavenge free radicals (Matsuda et al. 2001). In addition, previous work in my laboratory demonstrated that GPF protects human keratinocytes against oxidative stress-induced cell damage via its antioxidant effects (Yao et al. 2013). However, little is known about the protective effects of GPF against UVB radiation. Therefore, the capacity of GPF to protect HaCaT cells against UVB-induced oxidative stress and cell damage was investigated, as well as the mechanisms underlying this protection.

2. Materials and Methods

2-1. Materials

GPF (Fig. 1A) was provided by Professor Sam Sik Kang (Seoul National University, Korea). N-acetyl cysteine (NAC), 2',7'-dichlorodihydrofluorescein diacetate (DCF-DA), (3-(4,5-dimethylthiazol-2-yl)-2,5-diphenyltetrazolium) bromide (MTT), Hoechst 33342 dye and propidium iodide (PI) were purchased from Sigma Chemical Company (St. Louis, MO, USA). Diphenyl-1-pyrenylphosphine (DPPP) was purchased from Molecular Probes (Eugene, OR, USA). Primary antibodies against Bcl-2 and Bax were purchased from Santa Cruz Biotechnology (Dallas, TX, USA). Primary antibodies against caspase 3, caspase 9, and poly ADP-ribosyl polymerase (PARP) were purchased from Cell Signaling Technology (Beverly, MA, USA). All other chemicals and reagents were of analytical grade.

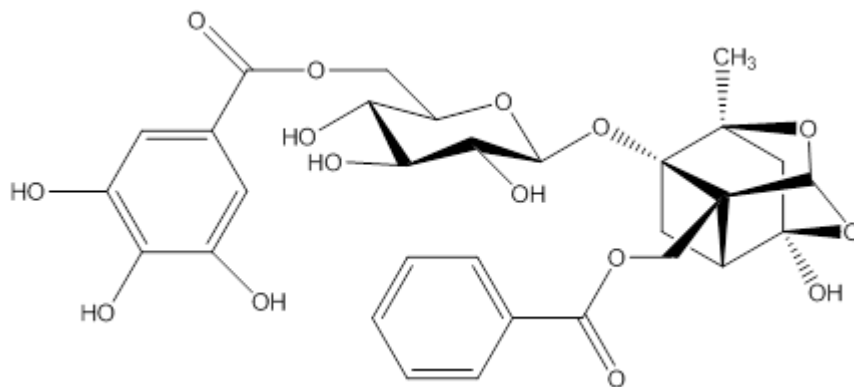


Figure 1A. Chemical structure of *GPF*

2-2. Cell culture

The human keratinocyte cell line HaCaT was obtained from the Amore Pacific Company (Gyeonggi-do, Korea) and maintained at 37°C in an incubator with a humidified atmosphere of 5% CO₂/95% air. The cells were cultured in RPMI 1640 medium containing 10% heat-inactivated fetal calf serum, streptomycin (100 µg/ml), and penicillin (100 units/ml).

2-3. UV/visible light absorption analysis

GPF was diluted 1:5000 (v/v) in dimethyl sulfide (DMSO). The ability of GPF to absorb UVB radiation was then evaluated by scanning the compound with UV/visible light in the 250–400 nm range. The absorption of specific wavelengths was measured using a Biochrom Libra S22 UV/visible spectrophotometer (Biochrom Ltd, Cambridge, UK).

2-4. Detection of intracellular ROS

The DCF-DA method was used to detect intracellular ROS levels in HaCaT cells (Rosenkranz et al. 1992). The level of intracellular ROS was detected using a FACSCalibur flow cytometer (Becton Dickinson, Mountain View, CA, USA). Cells were seeded in plates at a density of 1.0×10^5 cells/ml. Sixteen hours later, they were treated with 20 µM GPF or 2 mM NAC. After 1 h incubation at 37°C, the cells were exposed to UVB radiation at a dose of 30 mJ/cm². Twenty four later, the cells were loaded for 30 min at 37°C with 40 µM DCF-DA, the supernatant was removed by suction, and the cells were trypsinized and washed with PBS. Fluorescence of DCF-DA-loaded cells was measured using a flow cytometer and the CellQuest Pro software (Becton Dickinson). The level of intracellular ROS was also detected using spectrofluorometer. In these experiments, cells were treated with GPF, NAC, and UVB radiation as described above. The cells were then incubated for 24 h at 37°C, after which 50 µM DCF-DA was added and the plates were incubated for an additional 30 min at 37°C. The fluorescence of 2',7'-dichlorofluorescein (DCF) was detected and quantitated using a

PerkinElmer LS-5B spectrofluorometer (PerkinElmer, Waltham, MA, USA). For imaging-based analysis of intracellular ROS, cells were seeded on a chamber slide with 4-well plate at a density of 1×10^5 cells/ml. Sixteen hours after plating, the cells were treated with 20 μ M GPF; 1 h later, they were exposed to UVB radiation described above. After 24 h, 40 μ M DCF-DA was added to each well, and the cells were incubated for an additional 30 min at 37°C. The stained cells were then washed in PBS and mounted on a chamber slide in mounting medium. Images were collected using a confocal microscope and the Laser Scanning Microscope 5 PASCAL software (Carl Zeiss, Jena, Germany).

2-5. Single-cell gel electrophoresis (comet assay)

The degree of oxidative DNA damage was determined by the comet assay (Rajagopalan et al. 2003; Singh 2000). Two hours after UVB radiation, the cell suspension was mixed with 75 μ l of 0.5% low melting agarose (LMA) at 39°C, and the mixture was spread on a fully frosted microscope slide pre-coated with 200 μ l of 1% normal melting agarose. After solidification of the agarose, the slide was covered with another 75 μ l of 0.5% LMA, and then immersed in lysis solution (2.5 M NaCl, 100 mM Na-EDTA, 10 mM Tris, 1% Triton X-100, 10% DMSO, pH 10) for 1 h at 4°C. The slides were subsequently placed in a gel electrophoresis apparatus containing 300 mM NaOH and 10 mM Na-EDTA (pH 13) for 40 min, to allow for DNA unwinding and expression of alkali-labile damage. An electrical field was then applied (300 mA, 25 V) for 20 min at 4°C to draw the negatively charged DNA towards the anode. The slides were washed three times for 5 min at 4°C in a neutralizing buffer (0.4 M Tris, pH 7.5), stained with 40 μ l of ethidium bromide (50 μ g/ml), and observed under a fluorescence microscope. Images were analyzed using the Komet 5.5 software (Kinetic Imaging, Liverpool, UK). The percentage of total fluorescence in comet tails and the tail lengths were recorded from 50 cells on each slide.

2-6. Lipid peroxidation assay

Lipid peroxidation was assayed by colorimetric determination of the levels of 8-isoprostane, a stable end-product of lipid peroxidation, in medium from HaCaT cells (Beauchamp et al. 2002). A commercial enzyme immune assay (Cayman Chemical, Ann Arbor, MI, USA) was used to detect 8-isoprostane. Lipid peroxidation was also assessed by using DPPP as a probe (Okimoto et al. 2000). DPPP reacts with lipid hydroperoxides to yield a fluorescent product, DPPP oxide, thereby providing an indication of membrane damage. Cells were treated with 20 μ M GPF for 1 h, followed by exposure to UVB (30 mJ/cm²). Twenty four hours later, cells were incubated with 20 μ M DPPP for 30 min in the dark. Images of DPPP fluorescence were captured on a Zeiss Axiovert 200 inverted microscope at an excitation wavelength of 351 nm and an emission wavelength of 380 nm. The intensity of the DPPP fluorescence was then quantitated.

2-7. Protein carbonyl formation

After undergoing the GPF/UVB treatment described above, cells were incubated for an additional 24 h. The amount of protein carbonyl formation was determined using the OxiselectTM protein carbonyl enzyme-linked immunosorbent assay kit (Cell Biolabs, San Diego, CA, USA).

2-8. Cell viability assay

To evaluate the ability of GPF to protect human keratinocytes against UVB radiation, cells were pre-treated with 20 μ M GPF or 2 mM NAC for 1 h, after which they were exposed to UVB light and incubated at 37°C for 24 h. MTT stock solution (50 μ l; 2 mg/ml) was added to each well to yield a total reaction volume of 200 μ l. After the cells were incubated for 4 h, the media were aspirated. The formazan crystals in each well were dissolved in DMSO (150 μ l), and the absorbance at 540 nm was read on a scanning multi-well spectrophotometer

(Carmichael et al. 1987).

2-9. Nuclear staining with Hoechst 33342

Cells were treated with 20 μ M GPF or 2 mM NAC, and then exposed to UVB radiation 1 h later. After an additional 24 h incubation at 37°C, the DNA-specific fluorescent dye Hoechst 33342 (20 μ M) was added to each well, and the cells were incubated for 10 min at 37°C. The stained cells were visualized under a fluorescence microscope equipped with a CoolSNAP-Pro color digital camera (Media Cybernetics, Carlsbad, CA, USA). The degree of nuclear condensation was evaluated, and the apoptotic cells were counted.

2-10. Detection of sub-G1 hypodiploid cells

Apoptotic sub-G1 hypodiploid cells were quantified by flow cytometry (Nicoletti et al. 1991). Cells were pre-treated with GPF for 1 h, then exposed to UVB radiation and harvested 24 h later. Harvested cells were washed twice with phosphate buffered saline and fixed in 70% ethanol for 30 min at 4°C. Subsequently, the cells were incubated in 50 mg/ml PI solution and 50 μ g/ml RNase A in the dark for 30 min at 37°C. Flow cytometric analysis was performed using a FACS Calibur flow cytometer (Becton Dickinson). The numbers of sub-G1 hypodiploid cells were assessed based on histograms generated by CellQuest and ModFit computer programs.

2-11. Terminal deoxynucleotidyl transferase-mediated digoxigenin-dUTP nick end labeling (TUNEL) assay

The TUNEL assay was performed using an in situ cell death detection kit (Roche Diagnostics, Mannheim, Germany) according to the manufacturer's instructions. Briefly, image analysis for the TUNEL assay was achieved by seeding cells on chamber slides at a density of 1×10^5 cells/well. Sixteen hours after plating, cells were treated with GPF and

exposed to UVB 1 h later. For an additional 24 h, chamber slides were fixed with 4% paraformaldehyde for 1 h at 15–25 °C, and cells were permeabilized for 2 min in 0.1% sodium citrate solution containing 0.1% Triton X-100. After washing in PBS, sections were incubated with the TUNEL reaction mixture for 1 h at 37 °C. After washing with PBS, the stained cells were mounted onto a microscope slide in mounting medium (DAKO, Carpinteria, CA, USA). Cells were then observed under a fluorescent microscope (Olympus IX 70, Olympus Optical Co., Tokyo, Japan) and quantified.

2-12. Western blot analysis

Cell lysates were electrophoresed, and separated proteins were transferred onto nitrocellulose membranes (Bio-Rad, Hercules, CA, USA). The membranes were incubated with primary antibodies, followed by horseradish peroxidase-conjugated immunoglobulin G secondary antibodies (Pierce, Rockford, IL, USA). Protein bands were detected using an enhanced chemiluminescence Western blotting detection kit (Amersham Pharmacia Biotech, Piscataway, NJ, USA).

2-13. Statistical analysis

All measurements were performed in triplicate, and all values are expressed as the mean \pm the standard error. The results were subjected to an analysis of variance using Tukey's test to analyze differences between means. In each case, a p value < 0.05 was considered to be statistically significant.

3. Results

3-1. GPF absorbs UVB rays

The effect of GPF on the absorption of UVB was determined using an UV/visible spectrophotometer. GPF could absorb light in the range 280–320 nm, corresponding to the wavelength of UVB rays. Therefore, the light-absorbing properties of GPF might contribute to its cytoprotective effect against UVB radiation (Fig. 1B).

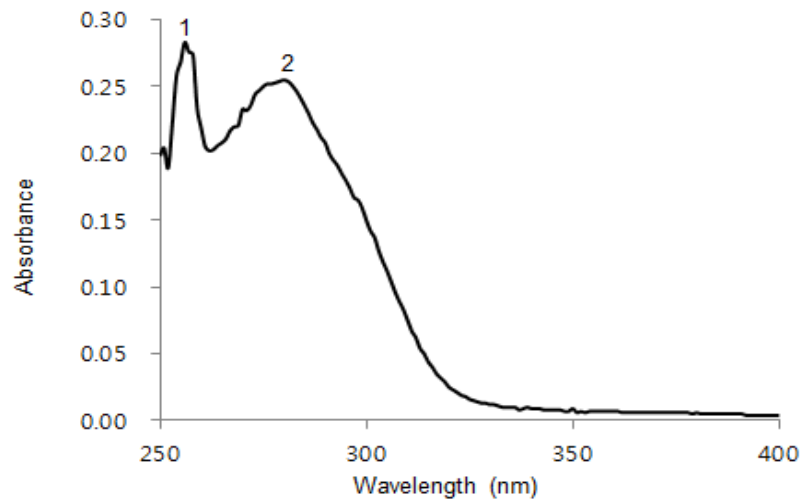


Figure 1B. GPF absorbs UVB light. UV/visible spectroscopic measurements were conducted in the spectral range from 250 to 400 nm. Peak 1, 257 nm; peak 2, 280 nm.

3-2. GPF scavenges ROS induced by UVB irradiation in HaCaT keratinocytes

The oxidation-sensitive fluorescent dye DCF-DA was used to detect intracellular ROS level. Flow cytometry was first utilized after DCF-DA staining to evaluate the ROS-scavenging activity of GPF in UVB-irradiated cells. In UVB-treated cells, GPF inhibited accumulation of UVB-induced intracellular ROS and a well-known antioxidant NAC was used as positive control (Fig. 2A). In addition, spectrofluorometric data exhibited that GPF scavenged the ROS in UVB-irradiated cells (Fig. 2B). In confocal microscopic images, the high fluorescence intensity representing UVB-induced ROS was significantly reduced upon treatment with GPF (Fig. 2C). These results demonstrate that GPF is a scavenger of intracellular ROS generated following UVB irradiation.

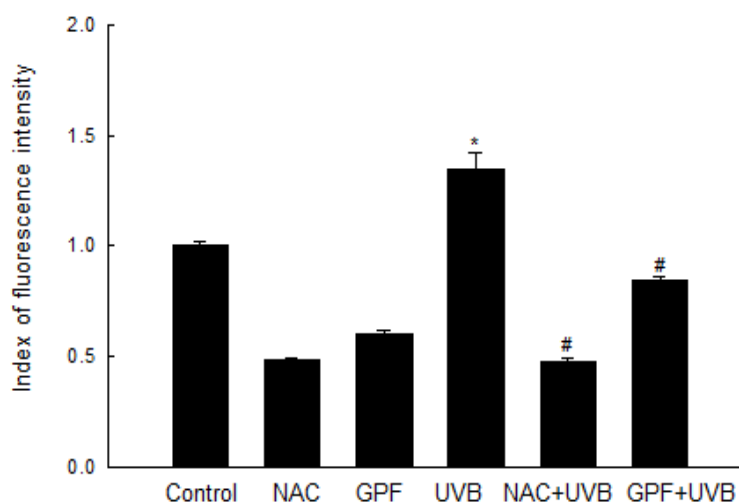
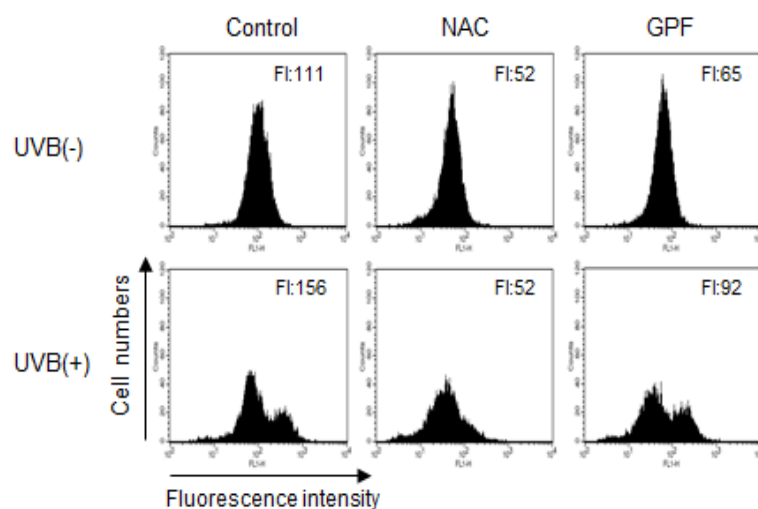


Figure 2A. Cells were treated with 20 μ M GPF or 2 mM NAC, exposed to UVB radiation (30 mJ/cm^2) 1 h later, and then incubated for an additional 24 h. Intracellular ROS were detected by flow cytometry after DCF-DA staining. *Significant difference relative to control cells ($p < 0.05$); #significant difference relative to UVB-irradiated cells ($p < 0.05$).

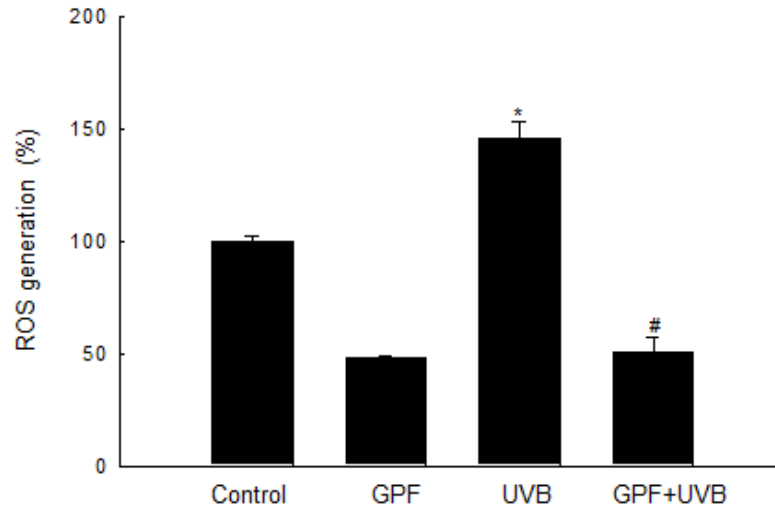


Figure 2B. Cells were treated with 20 μ M GPF, exposed to UVB radiation (30 mJ/cm^2) 1 h later, and then incubated for an additional 24 h. Spectrofluorometry was utilized to analyze the intracellular ROS levels after DCF-DA staining. *Significant difference relative to control cells ($p < 0.05$); #significant difference relative to UVB-irradiated cells ($p < 0.05$).

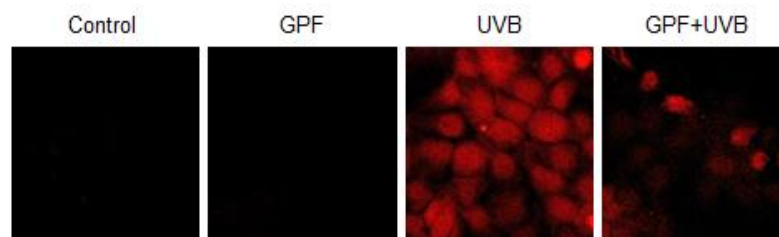


Figure 2C. After treated with 20 μ M GPF, cells were exposed to UVB radiation (30 mJ/cm^2) 1 h later, and then incubated for an additional 24 h. Intracellular ROS levels were detected by confocal microscopy after DCF-DA staining.

3-3. GPF attenuates UVB-induced macromolecular damage in HaCaT cells

UVB radiation induces multiple types of DNA damage, including cyclobutane pyrimidine dimers, 6-4 photoproducts, protein-DNA crosslinks, oxidative base damage, and single-strand breaks (de Gruijl et al. 2001). DNA strand breaks can be visualized under a microscope as comets; in these images, the length of the DNA tail length reflects the level of DNA lesions. UVB radiation induced a significant increase in DNA tail length and the percentage of damaged DNA in nuclear tails, as shown in the histogram in Figure 3A. However, pre-treatment with GPF prior to UVB exposure reduced the percentage of DNA in tails from 60% to 39%. Furthermore, GPF on its own did not increase the level of DNA lesions. These results demonstrate that GPF can attenuate the accumulation of DNA lesions in UVB-irradiated HaCaT cells.

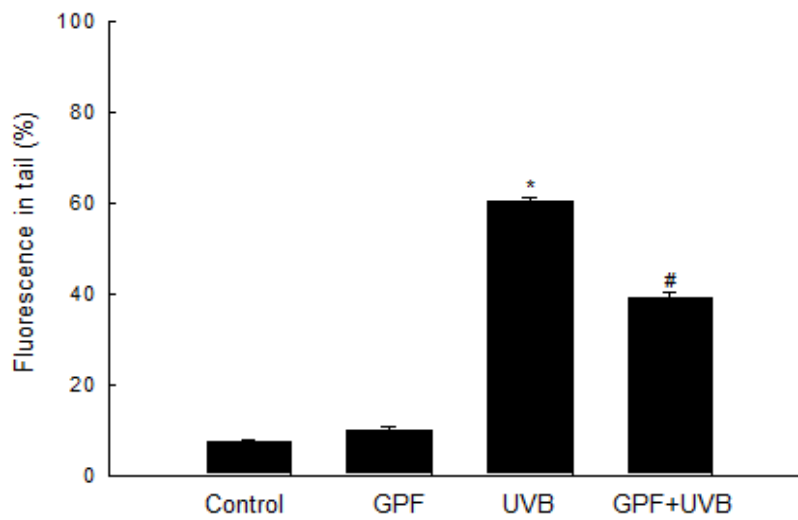
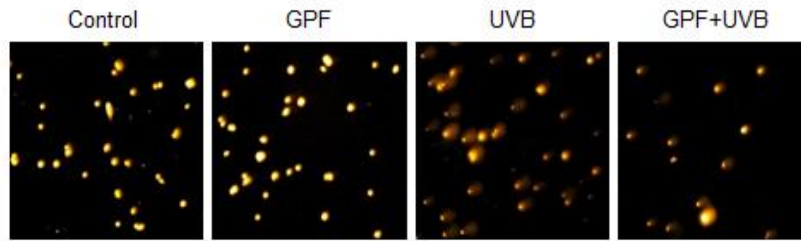


Figure 3A. HaCaT cells were treated with 20 μ M GPF for 1 h, and then exposed to UVB radiation. The comet assay was performed to assess DNA damage. Representative images and percentages of cellular fluorescence within comet tails are shown. *Significant difference relative to control cells ($p < 0.05$); #significant difference relative to UVB-irradiated cells ($p < 0.05$).

UVB irradiation can induce lipid peroxidation reactions in human keratinocytes (Punnonen et al. 1991). Lipid peroxidation can be monitored by measuring the amount of 8-isoprostane secreted by cells into the culture medium. UVB irradiation dramatically increased the level of 8-isoprostane, but pre-treatment of cells with GPF prior to UVB exposure abolished this increase (Fig. 3B). Likewise, the fluorescence intensity of DPPP, which reacts with lipid hydroperoxides to produce the highly fluorescent product DPPP oxide (Okimoto et al. 2000), was markedly increased by UVB radiation (Fig. 3C), but pre-treatment with GPF markedly decreased the DPPP intensity. This result indicates that GPF treatment reduced the level of lipid peroxidation, consistent with the results of the 8-isoprostane measurement.

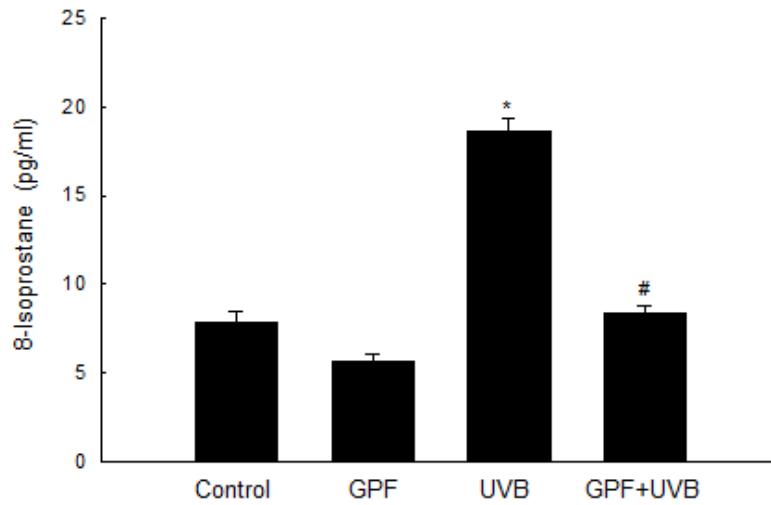


Figure 3B. Before exposed to UVB radiation, HaCaT cells were treated with 20 μ M GPF for 1 h. Lipid peroxidation was assayed by measuring 8-isoprostane levels which were released in conditioned medium. *Significant difference relative to control cells ($p < 0.05$); #significant difference relative to UVB-irradiated cells ($p < 0.05$).

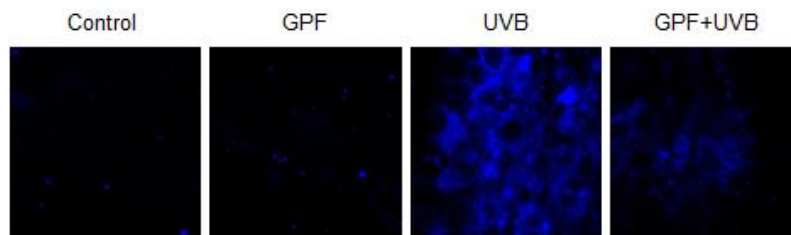


Figure 3C. HaCaT cells were treated with 20 μ M GPF for 1 h, and then exposed to UVB radiation. To evaluate lipid peroxidation level, lipid hydroperoxide detection was executed via fluorescence microscopy after the DPPP reaction.

Protein carbonylation is a biomarker for oxidative stress-induced protein damage (Dalle-Donne et al. 2003). The protein carbonyl level was significantly elevated in UVB-irradiated cells relative to control (Fig. 3D). GPF prevented UVB-induced protein carbonyl formation, consistent with its protective effects against DNA strand breaks and lipid peroxidation.

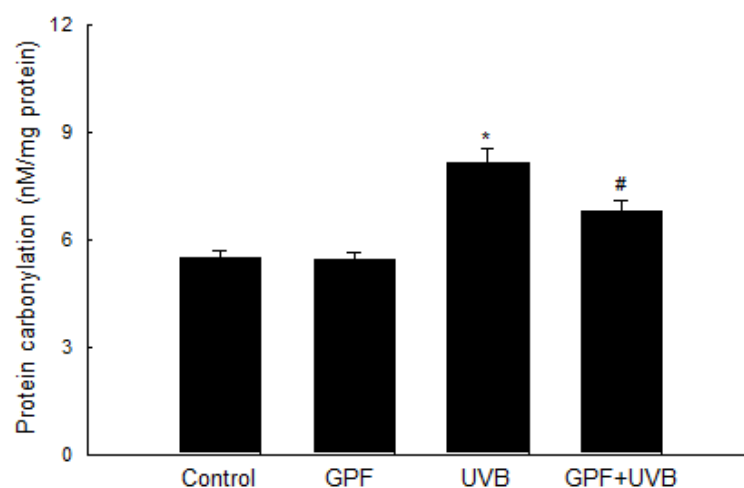


Figure 3D. HaCaT cells were treated with GPF at a concentration of 20 μ M in prior to UVB exposure. Protein oxidation was assayed by measuring the amount of carbonyl formation. *Significant difference relative to control cells ($p < 0.05$); #significant difference relative to UVB-irradiated cells ($p < 0.05$).

3-4. GPF protects HaCaT cells against apoptosis induced by UVB radiation

UVB radiation has been well-documented to trigger apoptosis and cell death in human keratinocytes (Schwarz et al. 1995). The effect of GPF on cell survival in UVB-irradiated HaCaT keratinocytes was investigated. Cell viability was determined using the MTT assay at 24 h after irradiation. GPF pre-treatment significantly increased viability, from 46% in the UVB-alone group to 55% in the GPF+UVB group, and NAC as positive control also increased viability decreased by UVB irradiation (Fig. 4A).

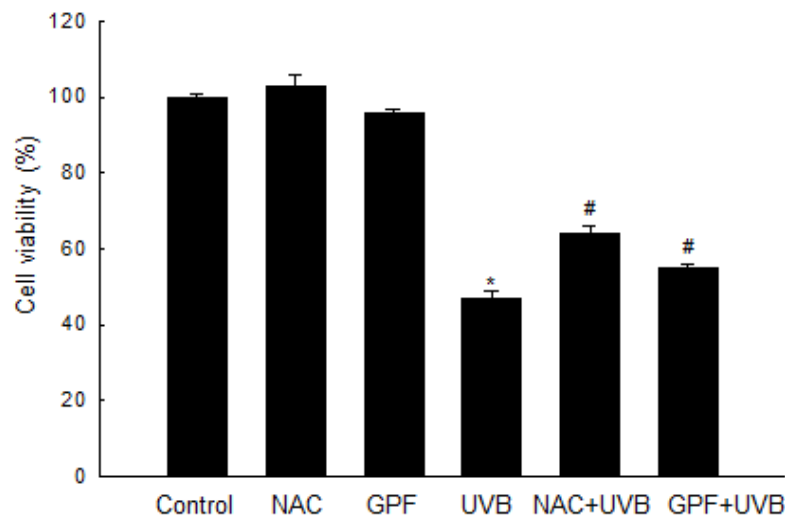


Figure 4A. Cells were treated with 20 μ M GPF or 2 mM NAC, and then exposed to UVB radiation 1 h later. After incubation for 24 h, cell viability was determined by the MTT assay. *Significant difference relative to control cells ($p < 0.05$); #significant difference relative to UVB-irradiated cells ($p < 0.05$).

Dynamic changes in the compaction of nuclear chromatin are characteristic of apoptotic execution (Wyllie et al. 1984). Nuclear fragmentation was visualized by staining cells with Hoechst 33342, and then examined under a fluorescence microscope. As observed in both images and the accompanying histogram, obvious nuclear fragmentation occurred in UVB-irradiated cells (apoptotic index 17) (Fig. 4B), but the rate of fragmentation was dramatically reduced by pre-treatment with GPF (apoptotic index 9). The cell population in the sub-G1 phase (apoptotic cells) was markedly increased up to 35% in UVB-irradiated cells compared to 4% of the control cells, however, pre-treatment with GPF decreased up to 26% in UVB-irradiated cells, as assessed by flow cytometry (Fig. 4C). Moreover, while the level of TUNEL-positive cells was higher in UVB-irradiated cells compared to control cells, the level of TUNEL-positive cells was significantly decreased in UVB-irradiated cells that were pre-treated with GPF (Fig. 4D).

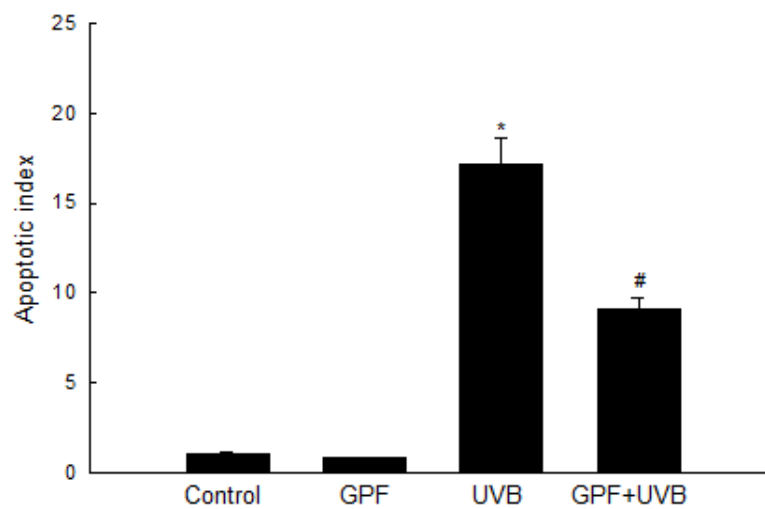
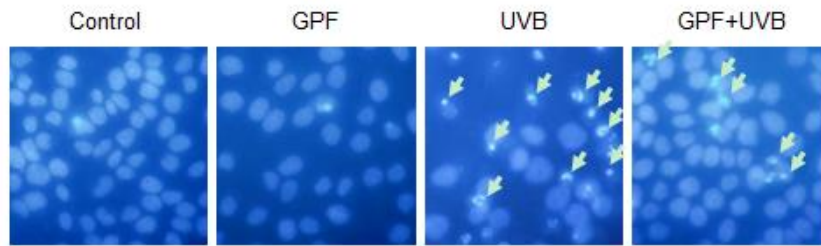


Figure 4B. In prior to UVB exposure, cells were pretreated with 20 μ M of GPF for 1 h. Apoptotic bodies (arrows) in cells stained with Hoechst 33342 dye were observed by fluorescence microscopy and quantitated. *Significant difference relative to control cells ($p < 0.05$); #significant difference relative to UVB-irradiated cells ($p < 0.05$).

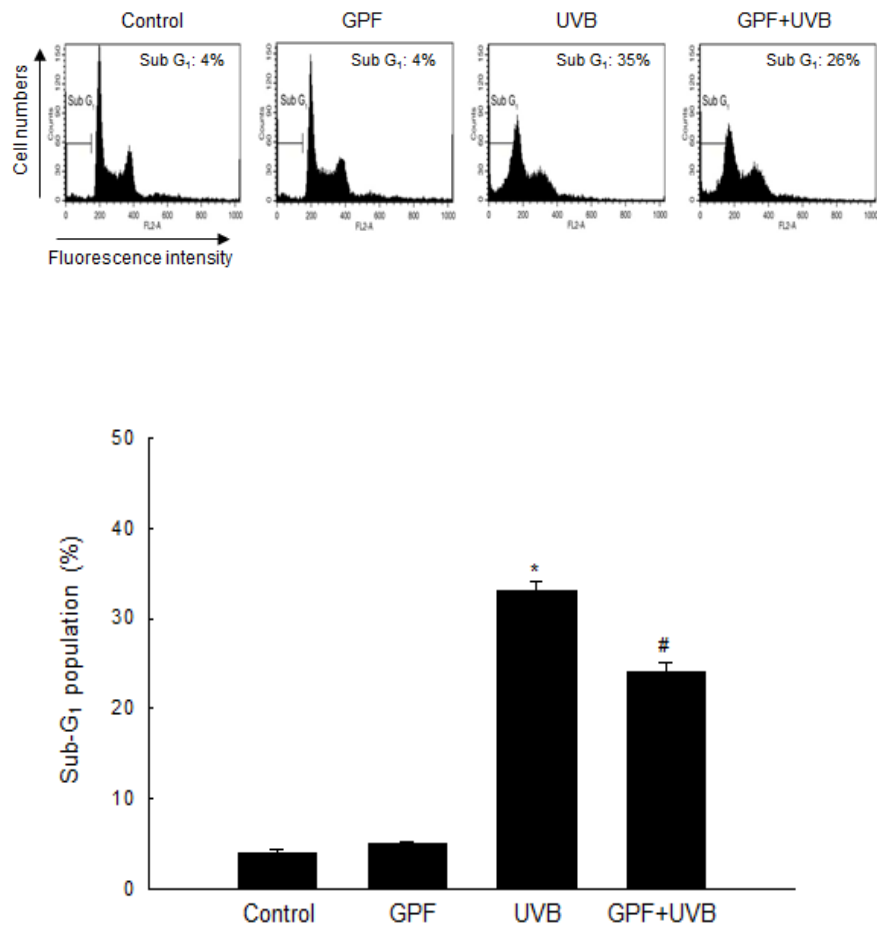


Figure 4C. Cells were incubated for additional 24 h, after the treatment of GPF (20 μ M) and then exposure to UVB. Sub-G₁ cells were detected by flow cytometry after PI staining. *Significant difference relative to control cells ($p < 0.05$); #significant difference relative to UVB-irradiated cells ($p < 0.05$).

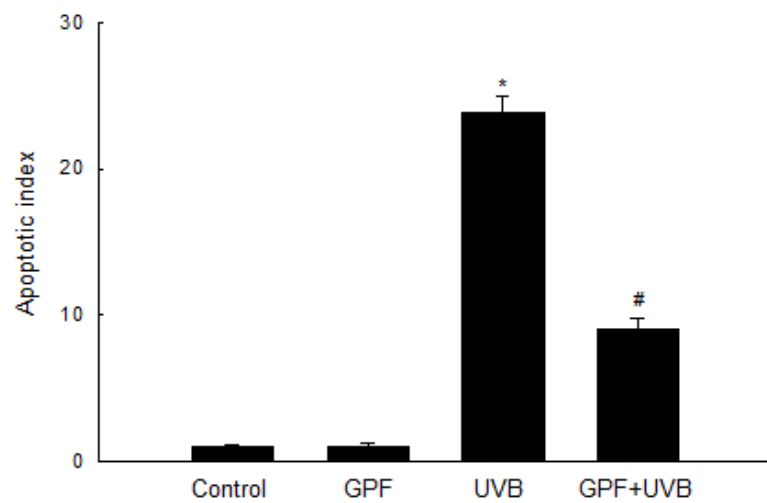
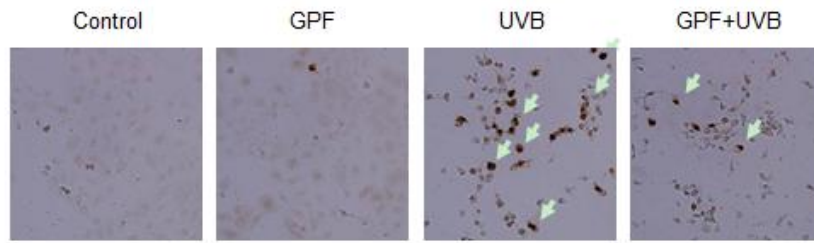


Figure 4D. Cells were treated with 20 μ M GPF or 2 mM NAC, and then exposed to UVB radiation 1 h later. After incubation for 24 h, apoptotic cells were detected by the TUNEL staining assay and quantified. *Significant difference relative to control cells ($p < 0.05$); #significant difference relative to UVB-irradiated cells ($p < 0.05$).

3-5. GPF prevents UVB-induced HaCaT cell death by regulating the mitochondria-related apoptotic pathway

To further understand the mechanism by which GPF protects against UVB-induced apoptosis, we measured the levels of proteins involved in mitochondria-mediated apoptosis. First, we monitored changes in expression of caspase 9 (a mitochondria-related caspase) and caspase 3 (an executive caspase). GPF pre-treatment decreased expressions of caspases and target protein PARP in UVB-irradiated cells (Fig. 5A). During the apoptotic process, both anti-apoptotic members (such as Bcl-2) and pro-apoptotic members (such as Bax) of the Bcl-2 family regulate apoptosis by inhibiting or promoting the permeabilization and disruption of the outer mitochondrial membrane (Mohamad et al. 2005). Because of their well-known roles in regulating mitochondrial apoptosis, we examined the levels of both Bcl-2 and Bax by Western blotting. Treatment of cells with GPF dramatically reversed the UVB-induced downregulation of Bcl-2 protein and upregulation of Bax protein (Fig. 5B). These results suggest that GPF protects cells against apoptosis by inhibiting the mitochondrial cell death pathway.

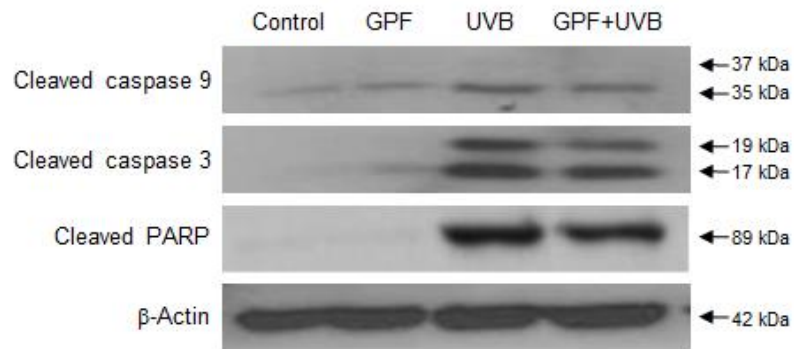


Figure 5A. Cells were incubated and harvest as pellet after UVB radiation. Cell lysates were electrophoresed, and cleaved caspase 9, cleaved caspase 3, cleaved PARP were detected using the appropriate antibodies. β -Actin is shown as a protein loading control.

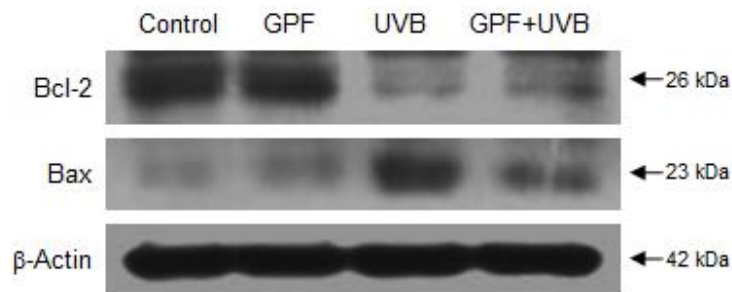


Figure 5B. Cells were incubated and harvest as pellet after UVB radiation. Cell lysates were electrophoresed, Bcl-2 and Bax were detected using the appropriate antibodies. β -Actin is shown as a protein loading control.

4. Discussion

GPF is a derivative of paeoniflorin, one of the principle active components in *Paeonia radix*. Recently, it is reported that GPF can scavenge ROS and rescue HaCaT cells from H₂O₂-induced macromolecular cell injury and even cell death (Yao et al. 2013). The results described in the current study provide the first demonstration that GPF can also reduce UVB-stimulated accumulation of excess intracellular ROS, safeguard HaCaT cells against macromolecular lesions, and prevent apoptosis by inhibiting the mitochondrial apoptotic pathway.

UVB, which constitutes only about 4–5% of UV radiation, is thought to be the most active constituent of solar radiation. UVB can reach the earth and penetrate the skin, causing a variety of adverse effects (Afaq 2011). In particular, UV-related skin carcinoma is of great concern, as its rates have been steadily increasing over recent years, and this trend is expected to continue in the future (F'guyer et al. 2003). Keratinocytes are the predominant cell population in the basal layer of the skin, and these cells are the primary targets of UVB (Grewe et al. 1995). The more hazard occurring in keratinocytes or skin tissues after UVB radiation is due to excessive ROS generation. Recent studies have implicated elevated intracellular H₂O₂ levels in the response to UVB radiation (Chang et al. 2002). In conjunction with previous work regarding the cytoprotective effects of GPF against H₂O₂ in HaCaT cells (Yao et al. 2013), the observations described above led us to our initial aim in this study: to investigate the cytoprotective effects of GPF against UVB-induced damage in HaCaT cells. DCF-DA staining, a widely used method for intracellular ROS detection, was used to examine the ability of GPF to scavenge intracellular ROS induced by UVB radiation. By flow cytometry, spectrofluorometry, and confocal image analysis, it showed that GPF pre-treatment of HaCaT cells indeed inhibited the UVB-induced elevation of ROS levels.

Currently, there is growing awareness that oxidative stress, which arises as a result of abnormal excessive ROS generation, leads to oxidative damage to macromolecules, including DNA, lipids, and proteins (Ray et al. 2012). Among the various types of damage, DNA lesions are the most critical for regulation of cell fate, not only because UVB can produce grievous DNA lesions both directly (through photochemical reactions) and indirectly (through oxidative stress), but also due to the well-documented contribution of UVB-induced DNA lesions to carcinogenesis and apoptosis (Ichihashi et al. 2003). In this study, it showed that GPF effectively attenuated DNA damage after UVB exposure. Outside the nucleus, unsaturated lipids on cell membranes can be transformed into lipid radicals, and then undergo lipid peroxidation, during UVB radiation (Nishi et al. 1991). Quantitation of 8-isoprostane levels, as well as DPPP oxide fluorescence, provides a reliable measure of UVB-provoked oxidative lipid damage in cell membranes. Proteins are also important targets for oxidative modifications. Carbonyl groups may be introduced into proteins either by oxidative cleavage, direct oxidation of specific amino-acid residues, or reactions with aldehydes produced during lipid peroxidation (Sander et al. 2002). Protein carbonylation is therefore a suitable biomarker for UVB-induced protein damage in human keratinocytes. Taken together, the results described here show that GPF significantly reduced UVB-induced macromolecular damage in HaCaT keratinocytes by decreasing the levels of DNA lesions, protein carbonylation, and the generation of both 8-isoprostane and DPPP oxide. These observations further substantiate the cytoprotective effect of GPF against UVB-induced oxidative stress in human keratinocytes.

UVB radiation leads to cell death, including necrosis and apoptosis via multiple cellular and molecular mechanisms. In addition to substantially protecting intracellular macromolecules, GPF can also rescue human keratinocytes from UVB-induced cell death. In parallel experiments, it showed that treatment of cells with NAC, a widely used ROS inhibitor, also reduced the rate of cell death.

The protective effect of GPF may be mediated by absorption of UVB photons. It was observed that GPF has an absorbance peak at a wavelength of 280 nm, which is within the UVB region of the spectrum. However, despite this physical property, attention was focused on determining the biochemical mechanism by which GPF protects keratinocytes against UVB-provoked programmed cell death, especially apoptosis. Pre-treatment with GPF reduced nuclear fragmentation and the formation of apoptotic bodies, both hallmarks of the apoptotic process, in UVB-irradiated HaCaT cells. Moreover, GPF also reversed the elevation of PARP cleavage by effector caspases such as caspase 3, another characteristic feature of apoptosis. Mitochondrial apoptosis, consisting of an initiator caspase (caspase 9) and an effector caspase (caspase 3), is also called the intrinsic death pathway. This pathway is distinct from the extrinsic pathway, which involves caspase 8 and cell-surface death receptors (Jeong and Seol 2008). The results show that UVB radiation triggered apoptosis in HaCaT cells via the intrinsic pathway, as demonstrated by the activation of caspase 9 and 3; both of these caspases were down-regulated following treatment with GPF. Proteins of the Bcl-2 family are critical regulators of mitochondria-dependent apoptosis. An imbalance between anti-apoptotic members (such as Bcl-2) and pro-apoptotic members (such as Bax) of this family usually occurs during apoptosis (Tsujimoto and Shimizu 2000). Here, the results of Western blotting demonstrated that GPF prevented UV-induced reduction in the level of an anti-apoptotic protein (Bcl-2) and elevation of the level of a pro-apoptotic protein (Bax). Thus, GPF can protect human keratinocytes against UVB-induced cell death by inhibiting the mitochondrial apoptotic pathway.

In summary, this study demonstrated that the natural antioxidant GPF could suppress excessive intracellular ROS generation triggered by UVB radiation in HaCaT cells. Moreover, GPF prevented cellular damage resulting from UVB radiation and also increased cell survival by inhibiting the mitochondrial apoptotic pathway. These data support the idea that GPF could be used as a therapeutic agent to treat ROS-related clinical diseases. For this

goal to be achieved, future studies should determine the biological efficacy of GPF, as well as the underlying mechanisms, in the context of other pathological processes both in vitro and in vivo.

All the main contents and experimental data are derived from the paper “*Cytoprotective effects of 6'-O-galloylpaeoniflorin against ultraviolet B radiation-induced cell damage in human keratinocytes*”, which was published on journal as “DOI: 10.1007/s11626-014-9747-0, *In Vitro Cellular & Developmental Biology–Animal*, April 2014”.

5. References

- Afaq F. Natural agents: cellular and molecular mechanisms of photoprotection. *Arch. Biochem. Biophys.* 508: 144-151; 2011.
- Alfadda A. A.; Sallam R. M. Reactive oxygen species in health and disease. *J. Biomed. Biotechnol.* 2012: Doi: 10. 1155/2012/936486; 2012.
- Beauchamp M. C.; Letendre É.; Renier G. Macrophage lipoprotein lipase expression is increased in patients with heterozygous familial hypercholesterolemia. *J. Lipid Res.* 43: 215-222; 2002.
- Carmichael J.; DeGraff W. G.; Gazdar A. F.; Minna J. D.; Mitchell J. B. Evaluation of a tetrazolium-based semiautomated colorimetric assay: assessment of chemosensitivity testing. *Cancer Res.* 47: 936-942; 1987.
- Chang H.; Sander C. S.; Müller C. S.; Elsner P.; Thiele J. J. Detection of poly (ADP-ribose) by immunocytochemistry: a sensitive new method for the early identification of UVB- and H₂O₂-induced apoptosis in keratinocytes. *Biol. Chem.* 383: 703-708; 2002.
- Dalle-Donne I.; Rossi R.; Giustarini D.; Milzani A.; Colombo R. Protein carbonyl groups as biomarkers of oxidative stress. *Clin. Chim. Acta* 329: 23-38; 2003.
- de Gruijl F. R.; van Kranen H. J.; Mullenders L. H. UV-induced DNA damage, repair, mutations and oncogenic pathways in skin cancer. *J. Photochem. Photobiol., B* 63: 19-27; 2001.
- F'guyer S.; Afaq F.; Mukhtar H. Photochemoprevention of skin cancer by botanical agents. *Photodermatol., Photoimmunol. Photomed.* 19: 56-72; 2003.
- Grewe M.; Gyufko K.; Krutmann J. Interleukin-10 production by cultured human

- keratinocytes: regulation by ultraviolet B and ultraviolet A1 radiation. *J. Invest. Dermatol.* 104: 3-6; 1995.
- Hampton M. B.; Orrenius S. Redox regulation of apoptotic cell death. *BioFactors* 8: 1-5; 1998.
- Hyun Y. J.; Piao M. J.; Zhang R.; Choi Y. H.; Chae S.; Hyun J. W. Photo-protection by 3-bromo-4, 5-dihydroxybenzaldehyde against ultraviolet B-induced oxidative stress in human keratinocytes. *Ecotoxicol. Environ. Saf.* 83: 71-78; 2012.
- Ichihashi M.; Ueda M.; Budiayanto A.; Bito T.; Oka M.; Fukunaga M.; Tsuru K.; Horikawa T. UV-induced skin damage. *Toxicology* 189: 21-39; 2003.
- Ikehata H.; Ono T. The mechanisms of UV mutagenesis. *J. Radiat. Res.* 52: 115-125; 2011.
- Jeong S. Y.; Seol D. W. The role of mitochondria in apoptosis. *BMB Rep.* 41: 11-22; 2008.
- Kang S. S.; Shin K. H.; Chi H. J. Galloylpaeoniflorin, a new acylated monoterpene glucoside from paeony root. *Arch. Pharmacol Res.* 14: 52-54; 1991.
- Kerksick C.; Willoughby D. The antioxidant role of glutathione and N-acetyl-cysteine supplements and exercise-induced oxidative stress. *J. Int. Soc. Sports Nutr.* 2: 38-44; 2005.
- Liu S.; Guo C.; Wu D.; Ren Y.; Sun M. Z.; Xu P. Protein indicators for HaCaT cell damage induced by UVB irradiation. *J. Photochem. Photobiol., B* 114: 94-101; 2012.
- Matsuda H.; Ohta T.; Kawaguchi A.; Yoshikawa M. Bioactive constituents of chinese natural medicines. VI. Moutan cortex.(2): structures and radical scavenging effects of suffruticosides A, B, C, D, and E and galloyl-oxypaeoniflorin. *Chem. Pharm. Bull.* 49: 69-72; 2001.
- Mohamad N.; Gutiérrez A.; Núñez M.; Cocca C.; Martín G.; Cricco G.; Medina V.; Rivera E.; Bergoc R. Mitochondrial apoptotic pathways. *Biocell* 29: 149-161; 2005.

- Nicoletti I.; Migliorati G.; Pagliacci M. C.; Grignani F.; Riccardi C. A rapid and simple method for measuring thymocyte apoptosis by propidium iodide staining and flow cytometry. *J. Immunol. Methods* 139: 271-279; 1991.
- Nishi J.; Ogura R.; Sugiyama M.; Hidaka T.; Kohno M. Involvement of active oxygen in lipid peroxide radical reaction of epidermal homogenate following ultraviolet light exposure. *J. Invest. Dermatol.* 97: 115-119; 1991.
- Okimoto Y.; Watanabe A.; Niki E.; Yamashita T.; Noguchi N. A novel fluorescent probe diphenyl-1-pyrenylphosphine to follow lipid peroxidation in cell membranes. *FEBS Lett.* 474: 137-140; 2000.
- Punnonen K.; Puntala A.; Ahotupa M. Effects of ultraviolet A and B irradiation on lipid peroxidation and activity of the antioxidant enzymes in keratinocytes in culture. *Photodermatol., Photoimmunol. Photomed.* 8: 3-6; 1991.
- Rajagopalan R.; Ranjan S. K.; Nair C. K. K. Effect of vinblastine sulfate on γ -radiation-induced DNA single-strand breaks in murine tissues. *Mutat. Res.-Genet. Toxicol. Environ. Mutag.* 536: 15-25; 2003.
- Ravanat J. L.; Douki T.; Cadet J. Direct and indirect effects of UV radiation on DNA and its components. *J. Photochem. Photobiol., B* 63: 88-102; 2001.
- Ray P. D.; Huang B. W.; Tsuji Y. Reactive oxygen species (ROS) homeostasis and redox regulation in cellular signaling. *Cell. Signal.* 24: 981-990; 2012.
- Rosenkranz A. R.; Schmaldienst S.; Stuhlmeier K. M.; Chen W.; Knapp W.; Zlabinger G. J. A microplate assay for the detection of oxidative products using 2',7'-dichlorofluorescein-diacetate. *J. Immunol. Methods* 156: 39-45; 1992.
- Sander C. S.; Chang H.; Hamm F.; Elsner P.; Thiele J. J. Role of oxidative stress and the antioxidant network in cutaneous carcinogenesis. *Int. J. Dermatol.* 43: 326-335; 2004.

- Sander C. S.; Chang H.; Salzman S.; Müller C. S.; Ekanayake-Mudiyanselage S.; Elsner P.; Thiele J. J. Photoaging is associated with protein oxidation in human skin *in vivo*. *J. Invest. Dermatol.* 118: 618-625; 2002.
- Savini I.; D'Angelo I.; Ranalli M.; Melino G.; Avigliano L. Ascorbic acid maintenance in HaCaT prevents radical formation and apoptosis by UV-B. *Free Radical Biol. Med.* 26: 1172-1180; 1999.
- Scandalios J. G. The rise of ROS. *Trends Biochem. Sci.* 27: 483-486; 2002.
- Schwarz A.; Bhardwaj R.; Aragane Y.; Mahnke K.; Riemann H.; Metze D.; Luger T. A.; Schwarz T. Ultraviolet-B-induced apoptosis of keratinocytes: evidence for partial involvement of tumor necrosis factor- α in the formation of sunburn cells. *J. Invest. Dermatol.* 104: 922-927; 1995.
- Singh N. P. Microgels for estimation of DNA strand breaks, DNA protein crosslinks and apoptosis. *Mutat. Res.-Fundam. Mol. Mech. Mutag.* 455: 111-127; 2000.
- Stahl W.; Sies H. Carotenoids and protection against solar UV radiation. *Skin Pharmacol. Physiol.* 15: 291-296; 2002.
- Tsujimoto Y.; Shimizu S. Bcl-2 family: life-or-death switch. *FEBS Lett.* 466: 6-10; 2000.
- Washida K.; Itoh Y.; Iwashita T.; Nomoto K. Androgen Modulators from the Roots of *Paeonia lactiflora* (*Paeoniae Radix*) Grown and Processed in Nara Prefecture, Japan. *Chem. Pharm. Bull.* 57: 971-974; 2009.
- Wyllie A.; Morris R.; Smith A.; Dunlop D. Chromatin cleavage in apoptosis: association with condensed chromatin morphology and dependence on macromolecular synthesis. *J. Pathol.* 142: 67-77; 1984.
- Yao C. W.; Piao M. J.; Kim K. C.; Zheng J.; Cha J. W.; Hyun J. W. 6'-O-Galloylpaeoniflorin Protects Human Keratinocytes Against Oxidative Stress-Induced Cell Damage. *Biomol.*

Ther. 21: 349-357; 2013.

6. Abstract in Korean

UVB 조사로 인한 인간 HaCaT 표피세포의 손상과 죽음에 대하여 분리된 6'-O-galloylpaconiflorin (GPF)의 세포보호 효과가 조사되었다. GPF는 UVB 조사로 인해 생성된 세포내 활성산소를 소거하는 능력을 보였다. 또한 GPF는 DNA 가닥 절단의 수와 지질 과산화의 생체 지표인 8-isoprostane의 레벨, 단백질 카르복실화의 레벨을 감소시킴으로 UVB로 인한 DNA, 지질과 단백질에 대한 산화적 거대분자의 손상을 경감시켰다. 더욱이 GPF는 미토콘드리아를 경유하는 죽음 경로를 억제함으로써 UVB로 인한 세포 죽음으로부터 HaCaT 세포가 회복될 수 있었다. 아울러, 이러한 결과들은 GPF가 ROS에 의한 피부 질환에 대한 의학적 치료 약물로써 사용될 가능성을 가지고 있다.

7. Acknowledgement

Firstly, I would like to show my great gratitude to my direct supervising professor Dr. Jin-Won Hyun. Her wise guidance, rigorous academic attitude on research and generous help in my daily life finally lead to my accomplishment on the Master degree thesis, which would be the precise wealth in my life.

In the next, I would like to express the gratitude to Prof. Hee-Kyong Kang and Prof. Young-Sang Koh, who instructed a lot on my graduation thesis and dissertation. All other professors providing me biochemical techniques and knowledges during my two-year study in Korea are also greatly appreciated.

Finally, I particularly appreciate Post Doctorate Mei-Jing Piao and Post Doctorate Ki-Cheon Kim for their thoughtful support, experimental and tactical suggestions. Moreover, my thankfulness is also given to all my labmates, Areum-Daseul Kim, Jian Zheng and Ji-Won Cha, for their kind assistance on my thesis achievement.